

Magnetic properties and microstructures of mischmetal-FeB-(Al, Ti and Al-Co) permanent magnets

K. Y. KO*,[‡]

Joule Laboratory, Department of Physics, Salford University, Salford M5 4WT, UK
E-mail: kyko@mail.ulsan-c.ac.kr

S. YOON

Department of Materials Science and Engineering, Ulsan University,
Ulsan City 680-749, South Korea

J. G. BOOTH, H. J. AL-KANANI

Joule Laboratory, Department of Physics, Salford University, Salford M5 4WT, UK

S. K. CHO

Department of Materials Science and Engineering, Ulsan University,
Ulsan City 680-749, South Korea

The magnetic characteristics of anisotropic MM-FeB- (Al, Ti and Al-Co) permanent magnets have been investigated by using hot-pressing and die-upsetting process. The best magnetic properties obtained in these studies were $H_C = 5.1$ kOe, $B_r = 5.4$ kG with $(BH)_{\max} = 5.1$ MGOe for hot-pressed MM-FeB-Al-Co magnets and $H_C = 3.6$ kOe, $B_r = 6.7$ kG, $(BH)_{\max} = 6.8$ MGOe for die-upset MM-FeB-Al-Co magnets. Higher squareness of demagnetization curve was obtained in anisotropic die-upset MM-FeB- (Al, Al-Co) magnets. X-ray diffraction and STEM investigations revealed that the higher magnetic properties in die-upset magnets were resulted from alignment of the *c*-axis along the die-upsetting direction. The magnetic anisotropy of the die-upset magnets and the densification of the hot-pressed magnets were increased by partial substitution of Al and Al-Co for Fe.

© 2002 Kluwer Academic Publishers

1. Introduction

The more abundant and inexpensive Mischmetal (MM) and Ferroboration (FeB) -substitutions, respectively, for Nd and Fe on the Nd-Fe-B magnets can provide low-cost rare-earth permanent magnets which can compete strongly with ferrites. Both La and Ce elements form a tetragonal $R_2Fe_{14}B$ compound [1] and the anisotropy field is maximum at the composition of about $(La_{0.4}Ce_{0.6})_2Fe_{14}B$ [2]. Melt-spun $MM_{16}Fe_{75}B_9$ [3] and MM-FeB [4] alloys produced with wheel velocity of 20–30 m/sec exhibited $H_C = 9.4$ kOe, $B_r = 6.2$ kG, $(BH)_{\max} = 8.1$ MGOe and $H_C = 5.7$ – 5.8 kOe, $B_r = 5.0$ – 7.9 kG, $(BH)_{\max} = 7.6$ – 8.9 MGOe, respectively. The addition of Co element in the $Nd_{15}(Fe_{77.5-x}Co_x)Al_2B_{5.5}$ permanent magnets increased the coercivity linearly in the range of 0–10 at.% Co preventing the formation of magnetic impurity phase [5]. Recently, Ko *et al.* [6] showed that the magnetic anisotropy in die-upset and the densification of the hot-pressed in MM-FeB- (Al) permanent magnets are increased by Al-substitution for Fe. In spite of possibility for practical use, MM-FeB permanent magnets have

been investigated by relatively small number of researchers. In this paper, the magnetic properties and microstructures of hot-pressed and die-upset MM-FeB- (Al, Ti and Al-Co) permanent magnets and effects of substitution of Al, Ti and Co for Fe are reported.

2. Experimental methods

MM-FeB- (Al, Ti and Co) alloys were melted in an argon arc furnace from 99.5% Al, 99.5% Ti, 99.5% Co, commercial grade mischmetal (MM) and 10wt% ferroboration with the chemical composition shown in Table I. The actual atomic compositions of the alloys fabricated are as follows:

TABLE I Chemical analyses of mischmetal and ferroboration

Ferroboration (FeB)							
Elements	Fe	B	C	Si	Al		
Wt%	85.5	9.0	1.0	4.0	0.5		
Mischmetal (MM)							
Elements	Ce	La	Nd	Pr	Fe	Ba	Others
Wt%	51.90	26.09	14.25	5.33	1.43	0.12	0.88

*Author to whom all correspondence should be addressed.

[‡]Present Address: Schools of Mechanical Engineering, West Campus, Ulsan College, Ulsan Metropolitan City, 680-749, South Korea.

Specimens	MM	Fe	B	Al	Ti	Co
MM-FeB	12.5	78.9	8.6	–	–	–
	15.0	77.0	8.0	–	–	–
MM-FeB-Al	12.5	77.9	8.6	2.0	–	–
	15.0	76.0	8.0	2.0	–	–
MM-FeB-Ti	12.5	76.9	8.6	–	1.0	–
	15.0	75.0	8.0	–	1.0	–
MM-FeB-Al-Co	12.5	71.9	8.6	2.0	–	5.0
	15.0	69.0	8.0	3.0	–	5.0

Small pieces of the crushed master alloy were put into quartz tube having a 0.7 mm hole in a high vacuum (10^{-6} torr) induction furnace and then melt-spun in an argon atmosphere ~ 70 mmHg using a rotating Cu wheel with 200 mm. The wheel speed was varied in the range of 10–45 m/s. The thicknesses and widths of the ribbons were about 25–40 μm and 2–3 mm respectively, depending on the wheel velocity. Ribbons for hot-pressed magnets were made with a surface velocity of about 40 m/sec. The melt-spun ribbons were crushed into powder with sizes less than about 150 μm under argon atmosphere using a mortar. Hot-pressed magnets were made into tablet forms of 4–5 mm high using a die with 8 mm bore, by 100 MPa pressure for 2–5 min. at about 700°C under argon atmosphere. MoS₂ lubricant was used to prevent the magnets from sticking to the punch and die. Die-upset magnets were made in an over-sized die with 20 mm bore. Die-upset magnets were made by re-pressing the hot-pressed magnets at about 730°C and 350 MPa under argon atmosphere.

The magnetic parameters were measured using a vibrating sample magnetometer (VSM) having a superconducting magnet with a maximum field of 12 T and/or Toei VSM B-H tracer at room temperature on samples pre-magnetized in a magnetic field of 2–3 kOe. X-ray diffractometry was used to determine the crystal struc-

ture of the master alloys, melt-spun ribbons, and hot-pressed and die-upset magnets at room temperature. Electron microscopy (Phillips 200CX, VG microscope HB601 STEM/Liverpool University, Joel 2000 TEM) and EPMA were used to examine their microstructures and phase analyses.

3. Results and discussions

Fig. 1 show the X-ray powder diffraction patterns of the melt-spun MM-FeB ribbons with function of wheel velocity. The major phase in all samples is the tetragonal R₂Fe₁₄B phase with lattice parameters of about $a = 8.77 \text{ \AA}$, $c = 12.20 \text{ \AA}$. As the wheel velocity increased, the peak intensities decreased and a completely amorphous state is assumed for the high velocity above 40 m/sec.

Fig. 2 show the high resolution STEM and EPMA results of the melt-spun ribbons with wheel velocity of about 25 m/sec appearing randomly oriented grains with sizes in the range of 30–100 nm. Some of the grains were of polygonal structures with sharp grain boundaries as in the hot-pressed Nd-Fe-B magnet [7] in contrast to the melt-spun Nd-Fe-B ribbons which have nearly spherical grains with curved grain boundaries [8]. Also, R-rich R-Fe-B second phase appeared with higher La concentration than matrix as shown in Fig. 2. All the phases appeared to have oxygen probably, strongly bound to the rare earth elements. This may support the possibility of an oxygen stabilized R-Fe-O phase that is magnetically anisotropic as suggested in Ref. [9, 10]. These results of microanalysis for ribbons are very similar to results of SEM for master ingots except that oxygen can not be detected by SEM. The presence of oxygen may cause a decrease in the coercivity if it forms paramagnetic oxides since it could act as a nucleation site for reverse domain [11]. Fig. 3 show X-ray diffraction patterns for hot-pressed and die-upset MM-FeB, MM-FeB-Ti, MM-FeB-Al

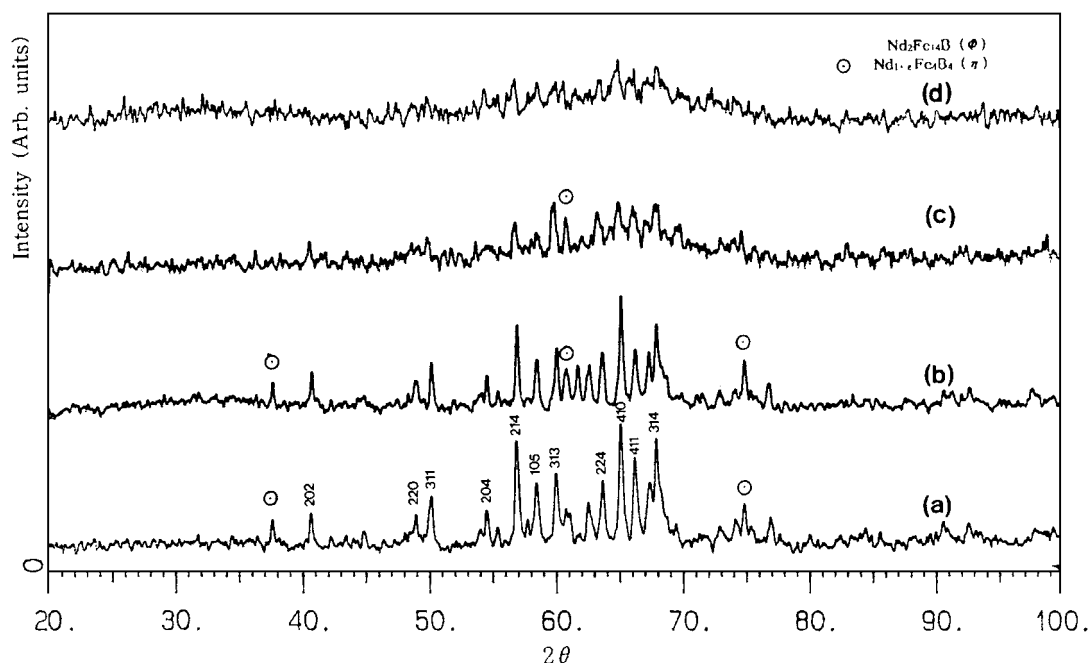


Figure 1 X-ray diffraction patterns of melt-spun MM-FeB ribbons with wheel velocity. (a) 10 m/sec, (b) 20 m/sec, (c) 25 m/sec, (d) 40 m/sec.

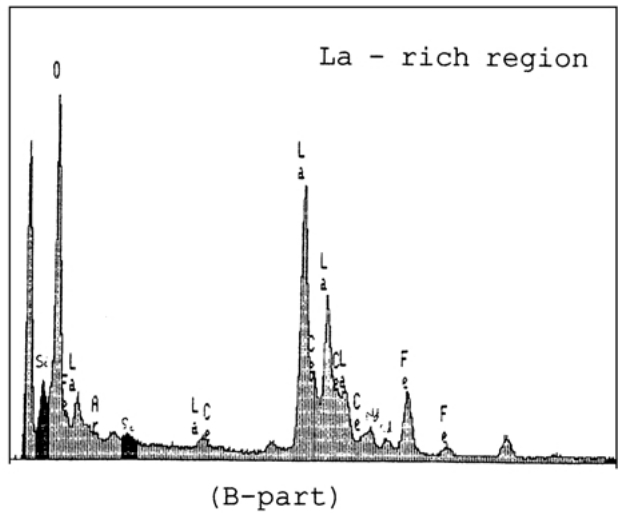
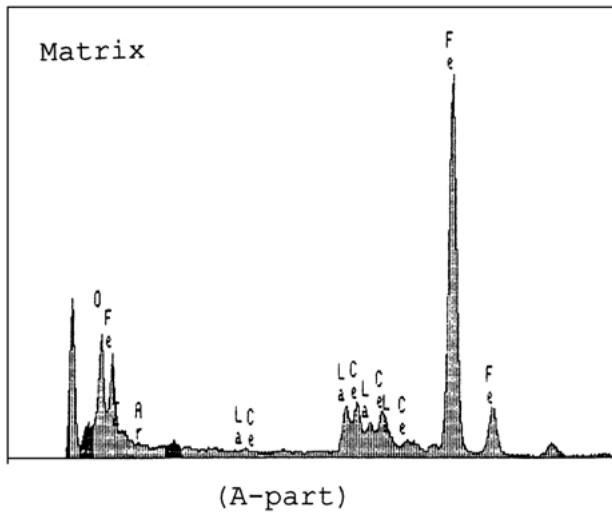
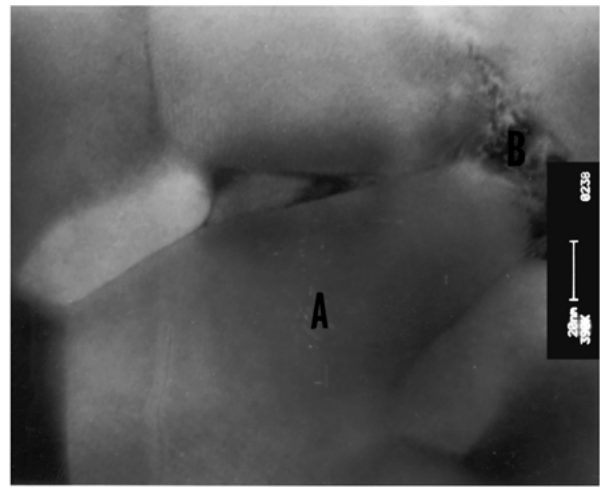
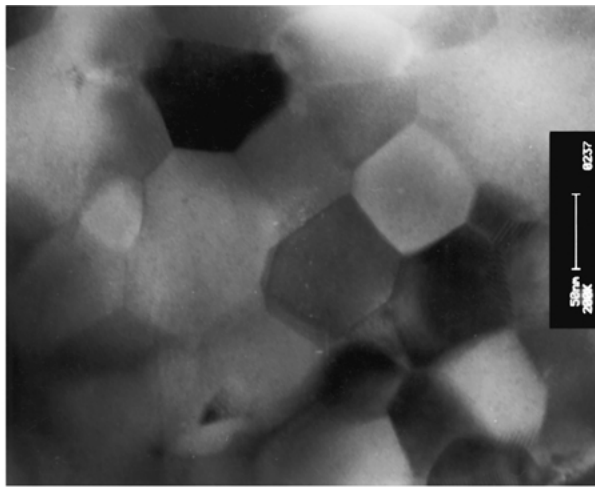


Figure 2 Transmission electron microscopy with microanalyses of melt spun MM-FeB ribbon with wheel velocity of 25 m/sec. (a) $\times 200,000$, (b) $\times 390,000$.

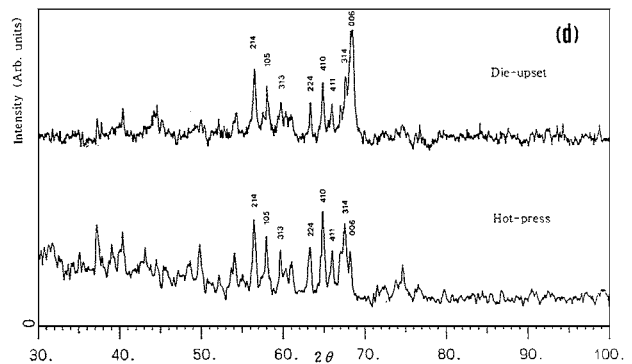
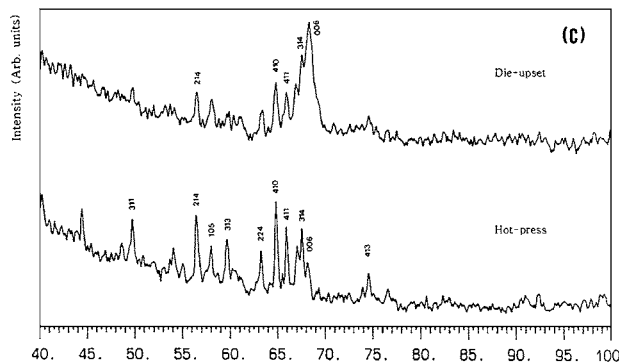
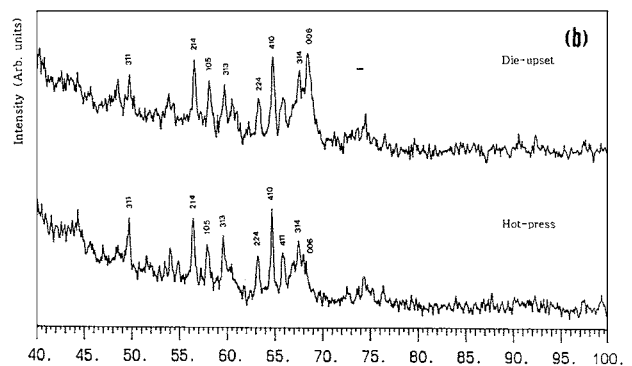
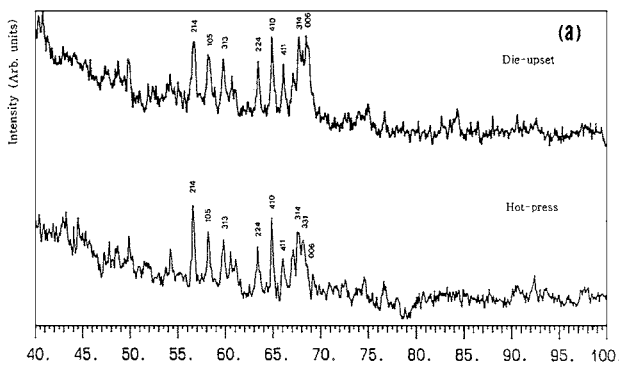


Figure 3 X-ray diffraction patterns of hot-pressed and die-upset (a) MM-FeB, (b) MM-FeB-Ti, (c) MM-FeB-Al and (d) MM-FeB-Co-Al magnets.

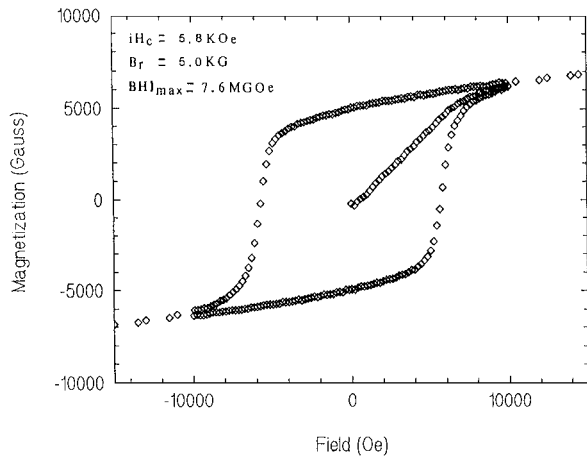
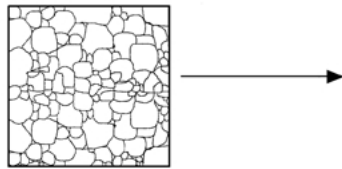


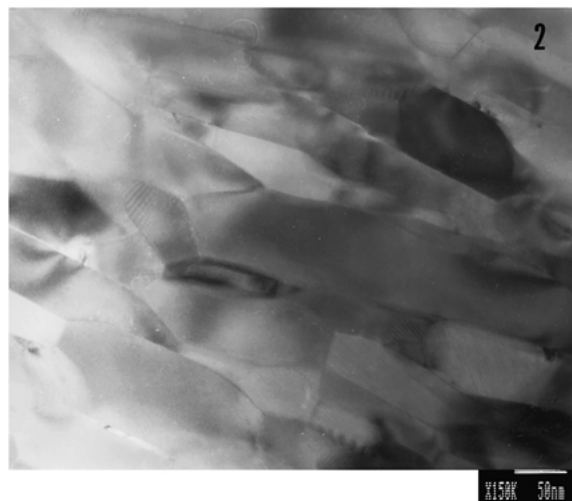
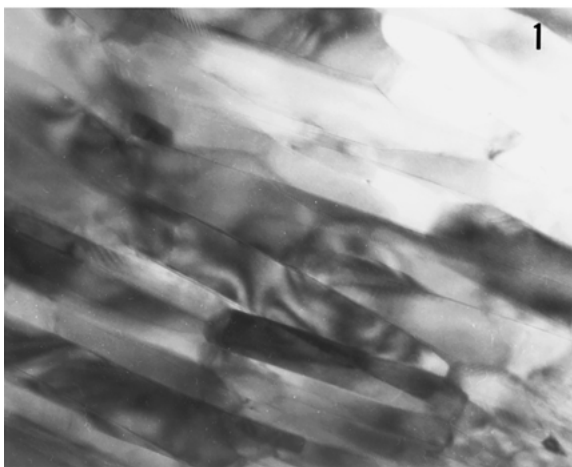
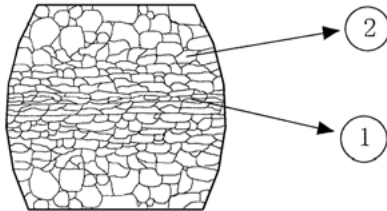
Figure 4 Hysteresis loops of melt-spun $MM_{12.5}Fe_{78.9}B_{8.6}$ ribbon with surface velocity of 25 m/sec.

and MM-FeB-Co-Al magnets. All but a few lines could be indexed as the tetragonal $R_2Fe_{14}B$ phase with lattice parameters of $a = 8.81 \text{ \AA}$ and $c = 12.21 \text{ \AA}$. It is also seen that the relative intensity of the (006) peak for the die-upset magnets is higher than that for the hot-pressed magnets. This indicates that c-axis alignment occurs during die-upset to the direction of die upsetting. Some extra peaks were common to all samples. These lines belong to second phases of R-rich phase and/or B-rich phase, probably RFe_4B_4 phase as shown in Figs 1 and 2. The optimal wheel velocity for the melt-spun ribbons to show good magnetic properties was found to be in the range of 20–30 m/sec. A typical hysteresis loop of the melt-spun $MM_{12.5}Fe_{78.9}B_{8.6}$ alloy ribbons is given in Fig. 4 showing $H_C = 5.8 \text{ kOe}$, $B_r = 5.0 \text{ KG}$ and $(BH)_{max} = 7.6 \text{ MGOe}$. The ratios of remanent to

Hot-pressed magnet



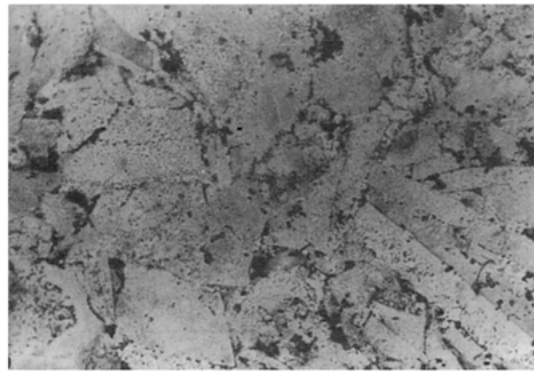
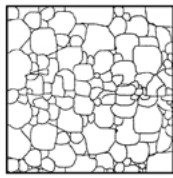
Die-upset magnet



(a)

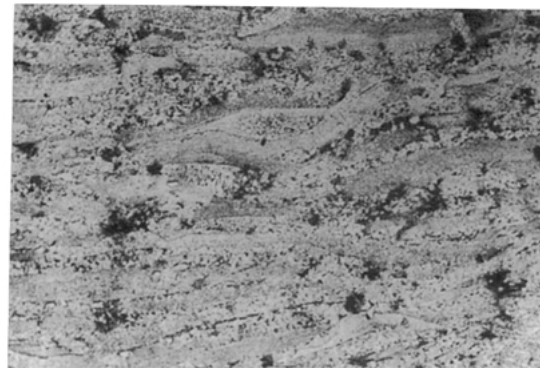
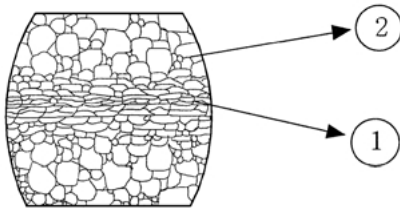
Figure 5 Optical and transmission electron microscopy of hot-pressed and die-upset (a) MM-FeB-Al and (b) MM-FeB-Co-Al magnets. (Continued.)

Hot-pressed magnet

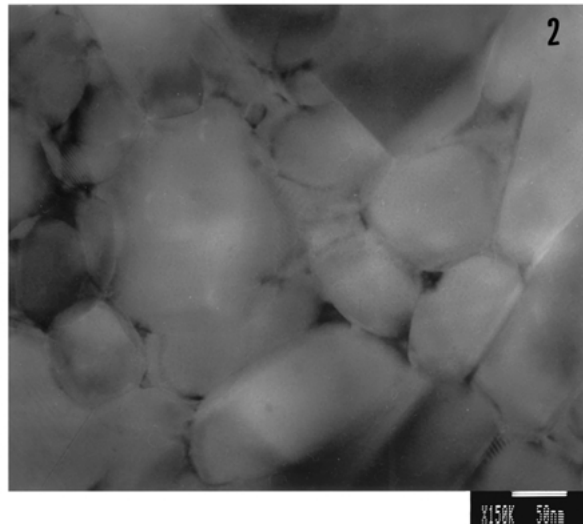
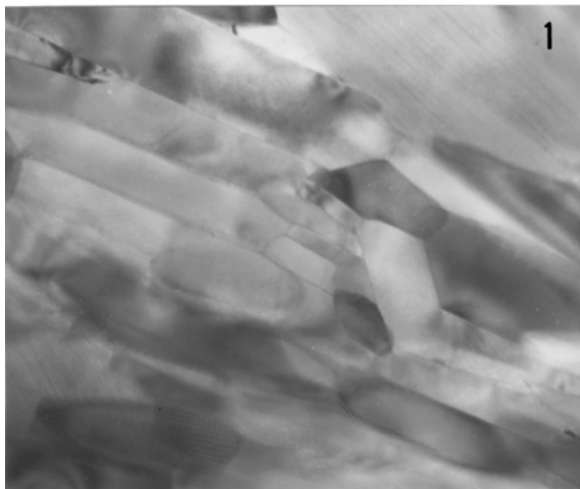


100 μm

Die-upset magnet



100 μm



(b)

Figure 5 (Continued.)

saturation magnetization (M_r/M_s) of the ribbons showed values in the range of 0.6–0.8, which is higher than those for (Ce, La)-Fe-B quenched ribbons [12] and heat-treated $MM_{17}Fe_{75}B_8$ ribbon [13]. It is reported that the high remanence might be due to the presence of Si contained in ferroboration since Si element keeps ultra-fine grain sizes [14]. The coercivities obtained were similar to those of (Ce, La)-Fe-B ribbons [3]. The densities of hot-pressed MM-FeB, MM-FeB-Al, MM-FeB-Co-Al and MM-FeB-Ti magnets were estimated to be about $7.23 \text{ g}\cdot\text{cm}^{-3}$, $7.24 \text{ g}\cdot\text{cm}^{-3}$,

$7.37 \text{ g}\cdot\text{cm}^{-3}$ and $7.17 \text{ g}\cdot\text{cm}^{-3}$, respectively. The height reductions by die-upsetting were measured as about 9.7%, 23%, 23% and 23% in MM-FeB, MM-FeB-Al, MM-FeB-Co-Al and MM-FeB-Ti magnets, respectively. Fig. 5a and b showed optical and STEM micrographs for hot-pressed and die-upset MM-FeB-Al and MM-FeB-Co-Al magnets. This shows that for the die-upset magnets grains are flattened in the directions perpendicular to the pressing direction. Typical demagnetization curves of the hot-pressed and die-upset MM-FeB-Al and MM-FeB-Co-Al

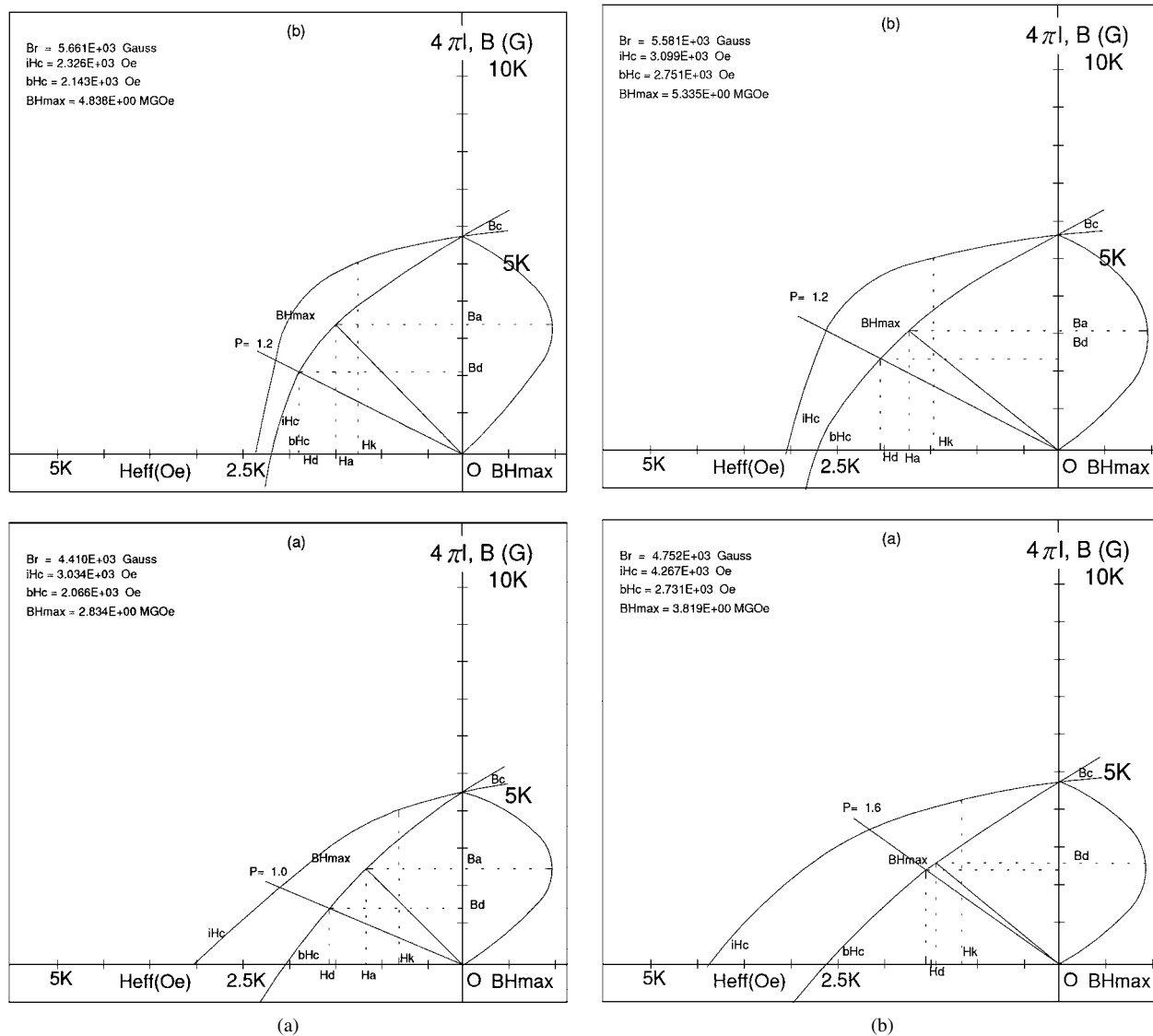


Figure 6 Demagnetization curves of hot-pressed and die-upset (a) MM-FeB-Al and (b) MM-FeB-Co-Al magnets.

magnets are given in Fig. 6a and b. The results for MM-FeB magnets were $H_C = 3.7$ kOe, $B_r = 5.0$ kG, $(BH)_{max} = 4.1$ MGOe for hot-pressed and $H_C = 2.6$ kOe, $B_r = 5.9$ kG with $(BH)_{max} = 4.1$ MGOe for die-upset. The MM-FeB-Al magnets gave $H_C = 5.1$ kOe, $B_r = 4.8$ kG with $(BH)_{max} = 3.3$ MGOe when hot-pressed and $H_C = 3.6$ kOe, $B_r = 6.4$ kG with $(BH)_{max} = 6.3$ MGOe when die-upset. The MM-FeB-Al-Co magnets gave $H_C = 5.1$ kOe, $B_r = 5.4$ kG with $(BH)_{max} = 5.1$ MGOe when hot-pressed and $H_C = 3.6$ kOe, $B_r = 6.7$ kG with $(BH)_{max} = 6.8$ MGOe when die-upset. These results are tabulated in Table II. The remanences of the die-upset MM-FeB, MM-FeB-Al, MM-FeB-Co-Al and MM-FeB-Ti magnets were improved by 19.6%, 29.5%, 16.7% and 8.7%, respectively, compared to the corresponding hot-pressed magnets. The coercivities of the die-upset MM-FeB, MM-FeB-Al, MM-FeB-Co-Al and MM-FeB-Ti magnets were improved by 40%, 23.3%, 27.9% and 13.2% than those of hot-pressed magnets, respectively. In the case of MM-FeB-Al magnets, Al substitution for Fe increased both of the remanence and coercivity by 3.6%

TABLE II Summary of magnetic parameters determined for the materials under investigation

Specimens	Parameters			
	Br (KG)	iHc (kOe)	bHc (kOe)	(BH) max (MGOe)
Hot-pressed magnets				
MM-FeB	4.6	3.0	2.1	2.9
MM-FeB-Al	5.0	3.7	2.5	4.1
MM-FeB-Ti	4.4	3.0	2.1	2.8
MM-FeB-Al-Co	4.8	5.1	2.5	3.3
MM-FeB-Ti	4.6	3.8	2.1	2.8
MM-FeB-Al-Co	5.3	4.8	3.0	4.3
MM-FeB-Al-Co	4.8	4.3	2.7	3.8
MM-FeB-Al-Co	5.4	5.1	3.3	5.1
Die-upset magnets				
MM-FeB	5.5	1.8	1.8	3.4
MM-FeB-Al	5.9	2.6	2.0	4.1
MM-FeB-Al	5.7	2.3	2.1	4.8
MM-FeB-Ti	6.4	3.6	2.9	6.3
MM-FeB-Ti	5.0	3.3	2.3	3.5
MM-FeB-Al-Co	5.4	4.0	2.7	4.1
MM-FeB-Al-Co	5.6	3.1	2.8	5.3
MM-FeB-Al-Co	6.7	3.6	3.1	6.8

and 27.8% in die-upset magnets, though it did not make much improvement in the hot-pressed magnets. The substitution of Al for Fe seems to increase the mechanical deformation and magnetic anisotropy during die-upsetting. In the case of MM-FeB-Co-Al magnets, Co-Al substitution for Fe showed improvement in remanence and coercivity; 4.3% and 43.3% respectively for hot-pressed magnets and 2.2% and 72.2% respectively for die-upset magnets. MM-FeB-Co-Al magnets exhibited higher magnetic properties than MM-FeB-Al magnets, in both hot-pressed and die-upset. Partial Co-substitution for Fe in MM-FeB-Al magnets results in increase in magnetic anisotropy and Curie temperature (580 K) as suggested in Nd-Fe (Co, Al)-B permanent magnet systems [5]. In the case of hot-pressed MM-FeB-Ti magnets, the coercivity was increased by 26.7% and the remanence was nearly unchanged compared with MM-FeB magnet. The remanence of the die-upset MM-FeB-Ti magnet was decreased by 9.1%, and coercivity was 83.3% higher than that of MM-FeB magnet. The small cracks existed in hot-pressed MM-FeB-Ti magnets and it might result in lower (BH) max values than those of MM-FeB magnets. The magnetic properties of MM-FeB-M alloys, in general, are much lower compared with Nd-Fe-B (C) permanent magnets [5]. This is mainly because of lower magnetocrystalline anisotropy of tetragonal (La, Ce)-Fe-B compounds [1]. Higher squareness (~ 0.8) of demagnetization curve of the die-upset MM-FeB-Al and MM-FeB-Co-Al magnet suggests that die-upsetting could be a useful tool for fabrication of anisotropic MM-FeB-(Al, Ti and Al-Co) magnets competing with ferrite systems. Bonded magnets were fabricated using polyamide binder. From SEM micrographs (not given in this paper), it was seen that densification was not satisfactory. Densities were about $5.5 \text{ g} \cdot \text{cm}^{-3}$ which are roughly 75% of attainable values in this systems. Bond magnets were magnetically isotropic with properties; $H_C = 2.3\text{--}3.5 \text{ kOe}$, $B_r = 3.1\text{--}4.0 \text{ kG}$ and $(BH)_{\text{max}} = 1.2\text{--}2.4 \text{ MGOe}$ depending on alloy composition.

4. Conclusions

The hot-pressed MM-FeB-Al-Co magnets showed $H_C = 5.1 \text{ kOe}$, $B_r = 5.4 \text{ kG}$ with $(BH)_{\text{max}} = 5.1 \text{ MGOe}$ and die-upset magnets $H_C = 3.6 \text{ kOe}$, $B_r = 6.7 \text{ kG}$, $(BH)_{\text{max}} = 6.8 \text{ MGOe}$. The higher magnetic properties of die-upset magnets over hot-pressed magnets

are mainly due to the alignment of the c -axis. Higher squareness (~ 0.8) of demagnetization curve was obtained in anisotropic die-upset (MM)-FeB-(Al, Al-Co) magnets. $H_C = 2.3\text{--}3.5 \text{ kOe}$, $B_r = 3.1\text{--}4.0 \text{ kG}$ and $(BH)_{\text{max}} = 1.2\text{--}2.4 \text{ MGOe}$ depending on alloy composition were obtained in bond magnets. The substitution of Co and Al for Fe resulted in increases of the densification in hot-pressed magnets and magnetic anisotropy of the die-upset magnets.

Acknowledgements

The authors are grateful to Prof. H. W. Davies (Sheffield University) and Dr. T. Davies (UMIST) for their help in making the hot-pressed samples and also, to H. Y. Lee (UMIST) for obtaining TEM micrographs. This research was supported partially by EPSRC and KOSEF program.

References

1. K. H. J. BUSCHOW, *Rep. Prog. Phys.* **54** (1991) 1123.
2. J. YAMASAKI, H. SOEDA, M. YANAGIDA and K. MOHRI, *Japan IEE Meeting on Magn.*, Sendai, Sept. MAG-85-101 (1985) 11.
3. J. YAMASAKI, H. SOEDA, M. YANAGIDA, K. MOHRI, N. TESHIMA, O. KOHMOTO, T. YONEYAMA and N. YAMAGUCHI, *IEEE Trans. Magn.* **MAG-22** (1986) 763.
4. K. Y. KO and J. G. BOOTH, *Proc. on 3rd International Symposium on Phys. of Magn. Mater.* **2** (1995) 771.
5. C. D. FUERST and E. G. BREWER, *J. Appl. Phys.* **70** (1991) 6444.
6. K. Y. KO, S. YOON and J. G. BOOTH, *J. Magn. Magn. Mater.* **176** (1997) 313.
7. R. K. MISHRA, *J. Appl. Phys.* **62** (1987) 967.
8. *Idem.*, *J. Magn. Magn. Mater.* **54-57** (1986) 450.
9. G. SCHNEIDER, E. HENIG, G. PETZOW and H. H. STADELMAIER, *Z. Metallkunde* **78** (1987) 695.
10. G. C. HADJIPANAYIS, A. TSOUKATOS, J. STRZESZEWSK, G. J. LONG and O. A. PRINGLE, *J. Magn. Magn. Mater.* **78** (1989) L1.
11. L. EYRING, in "Handbook on the Physics and Chemistry of Rare Earths," edited by K. A. Gschneidner and L. Eyring (North-Holland, Amsterdam, 1979).
12. J. J. CROAT, J. F. HERBST, R. W. LEE and F. E. PINKERTON, *J. Appl. Phys.* **55** (1984) 2078.
13. W. GONG and G. C. HADJIPANAYIS, *ibid.* **53** (1988) 3513.
14. G. B. CLEMENTS, J. E. KEEM and J. P. BRADLEY, *ibid.* **64** (1988) 5299.

Received 17 August 2000

and accepted 2 November 2001